Available online at https://link.springer.com/journal/42241
http://www.jhydrodynamics.com
Journal of Hydrodynamics, 2020, 32(3): 605-615
https://doi.org/10.1007/s42241-020-0938-9

The hydraulic performance of twin-screw pump *

Di Zhang, Li Cheng, Ying-yuan Li, Wei-xuan Jiao
School of Hydraulic, Energy and Power Engineering, Yangzhou University, Yangzhou 225009, China

(Received November 8, 2018, Revised February 11, 2019, Accepted February 27, 2019, Published online June 30, 2020)

Abstract: Based on the computational fluid dynamics (CFD) and the experiment technology, this paper presents a new type of the twin-screw pump for the water-supply and studies its hydraulic performance with the hydraulic performance test. The internal flow characteristics and the hydraulic performance of the twin-screw pump are numerically simulated. The CFD results show that at different heads, the screw pressure gradually increases from the inlet end face along the axial direction of the screw to the outlet end face. The pressure distribution in the screw groove is relatively uniform, the screw clearance and the meshing area pressure are different from the screw groove pressure distribution. Under the same working condition of the head, the pressure distributions in the screw below and above the design speed are the same as the pressure distribution at the design speed, and with the range of the pressure value quite close. As the rotating speed increases furthermore, the flow rate and the volume efficiency of the pump both increase. At different rotating speeds, the velocity distributions along the axial direction of the screw are similar. A test rig is built, which consists of a closed-loop circuit, and the test results are found in good agreement with the CFD predictions. The experimental results show that the flow rate-head curves of the twin-screw pumps are similar at different rotating speeds. The research shows that the designed twin-screw pump enjoys a higher volumetric efficiency and a lower shaft power when the axial clearance is 0.08 mm-0.12 mm. When the clearance is 0.1 mm, the volumetric efficiency is the highest.

Key words: Twin-screw pump, screw-rotor profile, hydraulic characteristics, screw clearances

Introduction

As a positive displacement pump, a twin-screw pump enjoys many advantages, including the stable transmission medium, the low pressure pulsation, the low noise, the long life, and the reliable operation. Therefore, it is of great significance to develop a twin-screw pump with a reliable operation and low vibrations for the farmland irrigation and drainage. Li[1] reviews the compositions of the screw pump, various types of structures and the calculation of the generation and the performance of the tooth profile. Yan et al.[2] analyzed difference in performance of 2-3 lobe combination of twin-screw pumps with different rotor profiles. The comparison of results obtained with two rotor profiles gave an insight on the advantages and disadvantages of each of them. Liu et al.[3] studied the influence of working fluid, pressure difference and pump rotating speed on the performance of multistage electrical submersible twin-screw pump, and an existing model to predict leakage flow of the single stage twin-screw pump was improved by extending the application for the multistage pumps. An et al.[4], Wang et al.[5] and Li et al.[6] performed a three-dimensional motion simulation analysis and a profile optimization for the rotor of the screw pump. It is shown that the modified involute tooth profile is an ideal profile with comprehensive features such as the sealing performance, the force transmission performance, and the process performance. Chen et al.[7] proposed an arc-corrected profile for the existing twin-screw pump profiles to avoid the point contact and effectively extend the service life of the pump. Tang and Zhang[8], Yan et al.[9] established a flow dynamics model based on the computational fluid dynamics (CFD) with a static grid, proposed a leak model for the twin-screw pump, and optimized the tooth profile. Ohbayashi et al.[10] outlined an approach of analyzing the balance among the geometrical pumping speed, the net throughput and the leaks. The cases of three kinds of clearances inside the screw pump were calculated and results were compared with the experiment with respect to the pump performance. Zhang et al.[11] conducted a large number of

* Project supported by the National Natural Science Foundation of China (Grant No. 51779214).
Biography: Di Zhang (1994-), Male, Ph. D. Candidate,
E-mail: dx120180054@yzu.edu.cn
Corresponding author: Li Cheng,
E-mail: chengli@yzu.edu.cn

experiments in accordance with the high-pressure water supply requirements of the screw. The results show that in order to ensure the balance of the axial forces, the screw must be a double-suction structure and be symmetrically arranged in a left-handed or right-handed manner. Hu et al.[12] established a theoretical model to evaluate the twin-screw pump clearance, the total pump volumetric flow, and the return flow in the power consumption for various pressure differentials and gas clearance fractions. Model predictions were found in good agreement with the experimental data. Liu et al.[13] developed an analytical model to predict the multi-phase performance of the twin-screw pump and to simulate the leakage flow in the clearance, which shows that the analytical model prediction and the experimental data are well matched. Zhang et al.[14-16] used the clearance leakage theory of hydromechanics to establish the differential pressure flow and shear flow model of the leakage in the pump chamber, analyzed the leakage of the screw cylinder wall clearance and the meshing clearance, respectively, and obtained an expression of the different clearance leakage of the screw pump. Patil[17], Yin et al.[18] studied the steady state and transient properties under different working conditions. They discussed the influence of the gas void fraction on the performance of the two-phase screw pump. Wang[19], Chu et al.[20] used the software Fluent to perform the CFD calculations on the designed twin-screw pump to obtain the velocity distribution, the pressure distribution and the stress field of the flow field. The effects of the fluid viscosity, the rotor speed, and the eccentricity of the screw pump on the flow field were analyzed. It is shown that there are significant pressure gradients in the flow passage, and the pressure increases gradually along the flow direction of the medium. This paper focuses on the research and development of the twin-screw pumps, including a screw rotor profile design, the hydraulic characteristics of the twin-screw pump and the effects of the speed and the screw clearance on the performance of the pump. At the same time, the hydraulic performance test of the twin-screw pump is carried out to reveal the hydraulic characteristics of the twin-screw pump and to broaden the application range of the twin-screw pump.

1. Research objects and simulation methods

1.1 *Research objects*

The twin-screw pump is an external meshing screw pump. It consists of a male rotor and a female rotor and a bushing for the two rotors. The fluid is conveyed through the intermeshing male and female rotors, with the male rotor of the pump driven by the prime mover, and the female rotor driven by the male rotor through a synchronous gear, as shown in Fig. 1. The medium pumped by the designed twin-screw pump is the water, and the Ω-type twin-screw pump is proposed to be in use. In view of the dynamic balance of the two rotors, a double-suction intake structure is used.

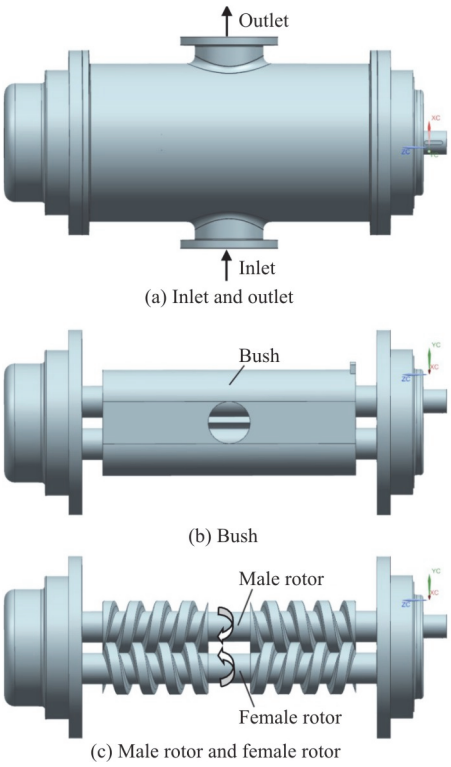

Fig. 1 Structure of twin-screw pump

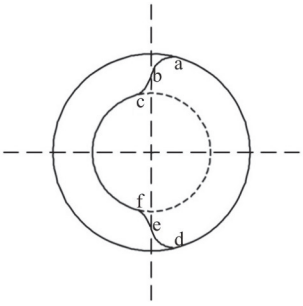

Fig. 2 End face profile of twin-screw pump

As shown in Fig. 2, the end face profile of the twin-screw pump consists of six segments: ab, bc, cf, fe, ed, and da. Let the radius of the pitch circle be a, the radius of the moving circle be b, θ is the angle at which the center of the moving circle is rotated relative to the center of the fixed circle. The segments ab and ed are epicycloid, governed by Eq. (1). The segments bc and fe are hypocycloid, governed by Eq. (2):

$$x=(a+b)\cos\theta_{ab}-r\cos\left[\left(\frac{a+b}{b}\right)\theta_{ab}\right],$$

$$y=(a+b)\sin\theta_{ab}-r\sin\left[\left(\frac{a+b}{b}\right)\theta_{ab}\right] \quad (1)$$

$$x=(a-b)\cos\theta_{bc}+r\cos\left[\left(\frac{b-a}{b}\right)\theta_{bc}\right],$$

$$y=(a-b)\sin\theta_{bc}+r\sin\left[\left(\frac{b-a}{b}\right)\theta_{bc}\right] \quad (2)$$

The CFD software SCORG and Pumplinx are used to calculate the hydraulic characteristics of the twin-screw pump and the effects of the screw clearance on the hydraulic characteristics. The design parameters of the twin-screw pump are as follows: the flow rate is greater than 180 m^3/h, the design head is 80 m, and the maximum shaft power is 50 kW. According to the design requirements, the related parameters of the twin-screw water pump profile are: the radius of the addendum circle $R_1=100$ mm, the radius of the pitch circle a=80mm, the radius of the root circle $R_2=60$ mm, and the rotor lead $T=80$ mm.

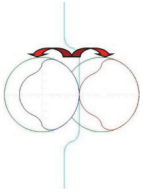

Fig. 3 (Color online) Rack line of male and female rotors

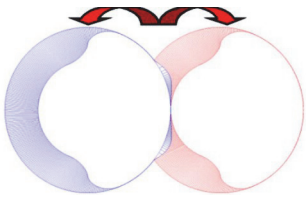

Fig. 4 (Color online) Surface meshes of screw rotor

1.2 *Numerical simulation*

The SCORG is used to mesh the grid for the twin-screw pump screw rotor, and the screw line coordinate data is imported into the SCORG. The twin-screw pump related design parameters are put in the rotor information column. The relevant parameters are set for the screw rack line to generate it, as shown in Fig. 3. The casing is divided conformal to the rotor. The number of output grid cells is 120 for each of the female rotor and the male rotor. The generated surface meshes and volume meshes are shown in Figs. 4, 5.

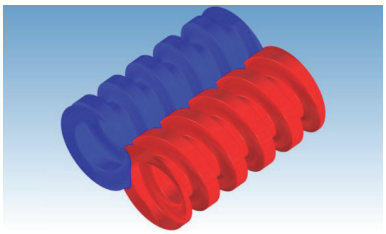

Fig. 5 (Color online) Volume meshes of screw rotor

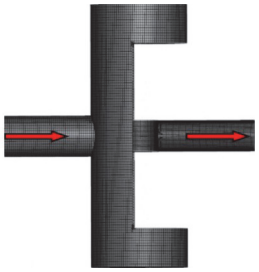

Fig. 6 (Color online) Mesh of inlet and outlet fluids

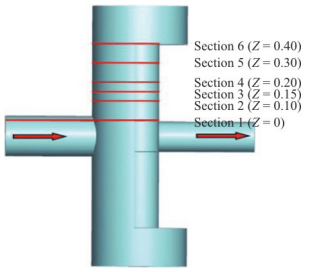

Fig. 7 (Color online) Fluid domain of twin-screw pump

The fluid domains of the pump inlet and outlet sections are meshed with Pumplinx. The general mesh model is selected. The relative dimensions are used, the maximum mesh size is set to 0.040, the minimum mesh size is set to 0.001, and the surface mesh size is set to 0.010, as shown in Fig. 6. A mesh-sensitivity study is carried out to determine the required mesh density. Several grids are considered, with the total number of cells ranging from 1.6×10^6 up to 3.8×10^6. No further refinement of results is obtained for grids with more than 2.6×10^6 cells.

In the interior of the twin-screw pump is a complicated turbulent flow. Due to the existence of the axial clearance, the radial clearance and the inter-lobe clearance, the pressure difference and the velocity difference are observed between different sealing chambers. Calculations are made using the commercial code Pumplinx. The numerical model is

based on the Reynolds-averaged Navier-Stokes (RANS) equations with the k-ω model to calculate the Reynolds stresses. Taking into account the specific conditions of the media transport process and the flow characteristics, the following assumptions are made: (1) The transport medium is incompressible, Newtonian fluid, (2) the flow field is stable and adiabatic, (3) the influences of the inertial force and the gravity can be ignored, and (4) the fluid fills the entire flow field. The reference pressure is 101 325 Pa

Under the above conditions, the Common template in Pumplinx is used as the calculation template, and the transmission medium is the water. The calculation cycle is set to 8 rotations of the screw, the pump inlet pressure is set to 0.1 MPa, and the pump outlet pressure is set to 0.88 MPa. By adjusting the pressure difference between the inlet and the outlet, the required flow rate is set. The rotating speed is 1 450 rpm.

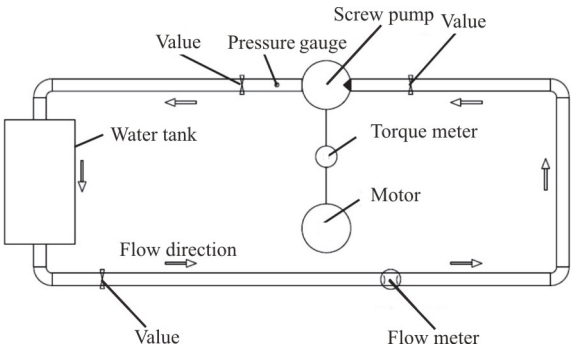

Fig. 8 Screw pump test rig

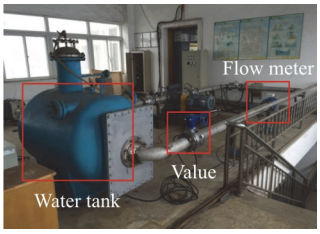

Fig. 9 (Color online) Overall layout of test rig

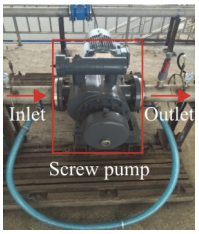

Fig. 10 (Color online) Screw pump segment

The import and export grids are imported into the Pumplinx screw rotor mesh file by SCORG. The assembly with the coordinate relationship is successful as shown in Fig. 7. To facilitate the following analysis, six sections are created as shown in the figure, Section 1 with $Z=0$, Section 2 with $Z=0.10$, Section 3 with $Z=0.15$, Section 4 with $Z=0.20$, Section 5 with $Z=0.30$, and Section 6 with $Z=0.40$. The screw axis is selected as Z axis (with the direction from the screw outlet end face to the screw inlet end face taken as positive), the vertical pump inlet and outlet direction is X axis (with the direction from the center of the drive screw to the center of the driven screw taken as positive), and the direction of the pump inlet and outlet is Y axis (with the direction from the pump inlet to the pump outlet taken as positive).

2. Hydraulic performance test of twin-screw pump

To verify the hydraulic performance of the designed twin-screw pump, a twin-screw pump test rig is built[21-22] (Figs. 8-10). The data measured in this test mainly include the screw pump speed, the inlet and outlet pressure difference (the head), the flow rate, and the shaft power. The hydraulic performances of the pump at five rotating speeds of 900 rpm, 1 100 rpm, 1 300 rpm, 1 450 rpm, and 1 600 rpm are, respectively, tested.

The efficiencies at corresponding operating points are calculated. The hydraulic performances at different rotating speeds are plotted in Fig.11. It can be seen from the figure that the hydraulic performances of the screw pump are basically the same at different speeds, that is, the relations between the flow rate and the head are the same at different speeds. In the range of the head in the test, the head of the screw pump shows a downward trend as the flow rate increases. Under the same head condition, there is a positive correlation between the pump flow rate and the speed. As the rotating speed increases, the flow rate of the pump increases.

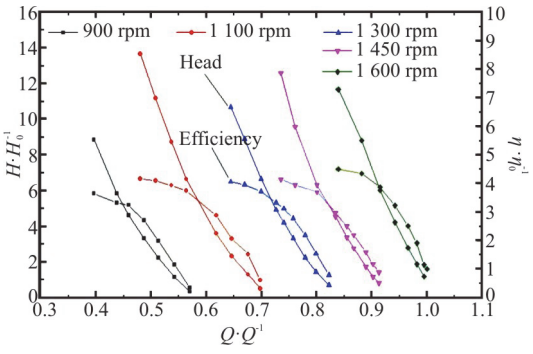

Fig. 11 (Color online) Hydraulic performance of screw pump at different rotating speeds in experiments

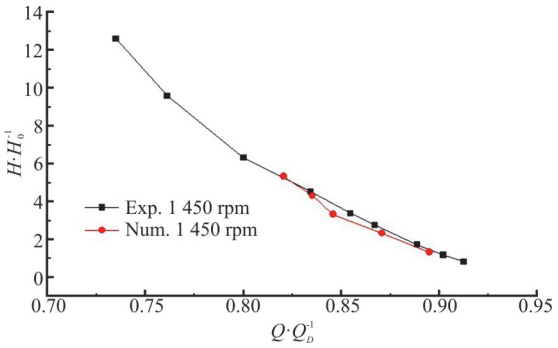

Fig. 12 (Color online) Hydraulic performance comparisons between results from experiment and CFD

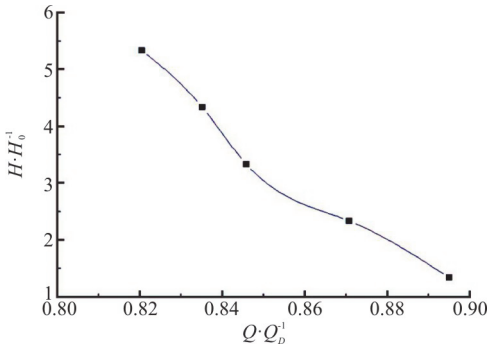

Fig. 13 Hydraulic performance (CFD)

The relationship between the flow rate and the total efficiency under different speed and head conditions is experimentally determined, as shown in Fig. 11, and it is indicated that at the design speed, the total efficiency of the screw pump increases with the decrease of the flow rate between $0.8Q_D$ - $0.9Q_D$. When the flow rate is lower than $0.8Q_D$, the efficiency increases slowly. At other speeds, one sees a similar trend, but with different operating conditions, the operating points are different, and the flow rate of the operating point increases with the increase of the speed. Figure 12 shows the comparison between the experimental results and the numerical simulation results, It is found that the error is small and the numerical simulation results are reliable.

3. Results and analysis of hydraulic characteristics

3.1 *Hydraulic characteristics of pump under different heads*

Figure 13 shows the flow rate-head relationship of a twin-screw pump (with H_0 being the minimum head). The head is obtained from the difference between the inlet pressure and the outlet pressure. $H_0 = 5.33$ is the design head condition. As can be seen from the figure, the flow rate of the twin-screw pump decreases as the head increases. Figure 14 shows the screw pressure distributions under five head conditions. It can be seen from the figure that the pressure change of the screw is in the same trend for different heads. The pressure increases gradually from the inlet end face along the axial direction of the screw to the outlet end face, and the pressure near the screw inlet end face is negative. The pressure distribution in the screw groove is relatively uniform, but the pressure distributions in the screw clearance and the meshing area are different from that in the screw groove.

Figures 15-17 show the pressure distributions of the screw end face at different screw sections. The average value of the screw pressure in the three sections reaches the maximum under the working condition of $H_0 = 5.33$, while the average value of the section screw pressure under the head $H_0 = 1.33$ is the smallest. That is, under different head conditions at the same section, the average pressure of the screw end surface increases with the increase of the head. Under different section conditions with the same head, the average value of the screw pressure in the Section 1 $(Z = 0)$ is the largest, that in the Section 3 $(Z = 0.15)$ is the second largest, and that in the Section 5 $(Z = 0.30)$ is the smallest. That is, the average value of the screw pressure gradually decreases from the screw outlet surface in the axial

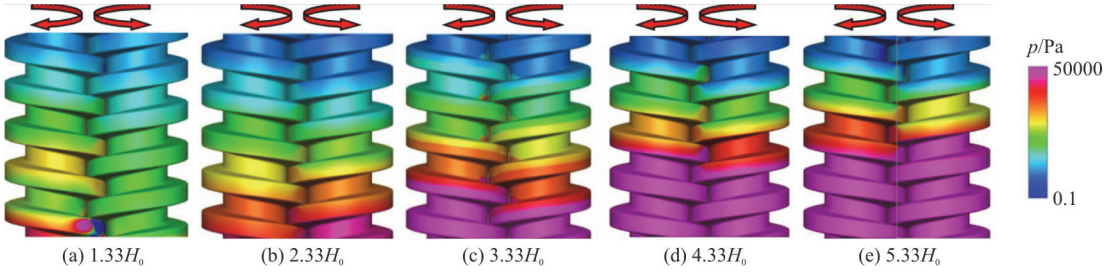

Fig. 14 (Color online) Pressure distributions of screw for different heads

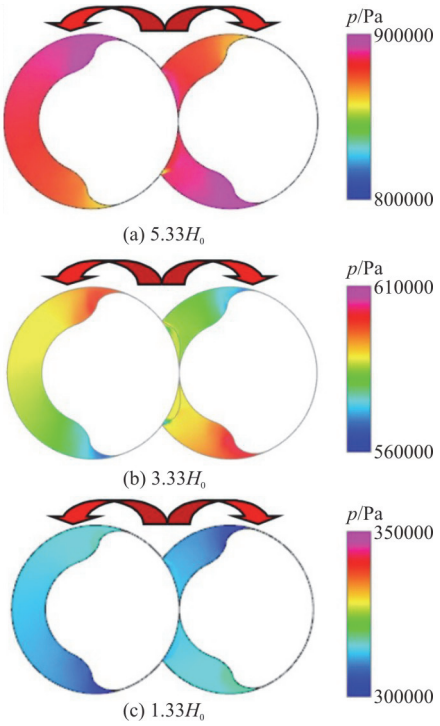

Fig. 15 (Color online) Screw pressure distribution in Section 1

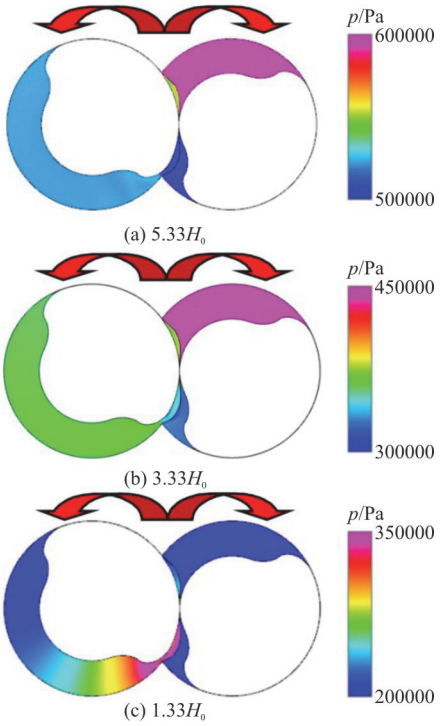

Fig. 16 (Color online) Screw pressure distribution in Section 3

direction of the screw. The pressure distribution in the screw groove in different sections and under different head conditions is relatively uniform, while the pressure in the clearance area and the meshing area between the rotor and the bush is different from that in the screw groove.

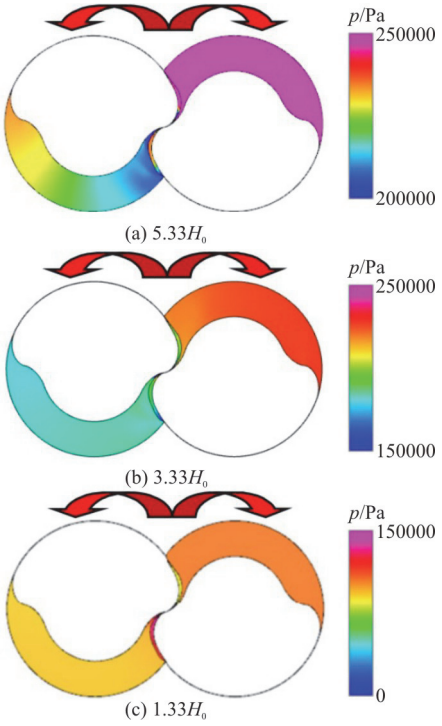

Fig. 17 (Color online) Screw pressure distribution in Section 5

Figure 18 shows the streamlines in the screw pump under different head conditions. It can be seen from the figure that under the working conditions of $H_0 = 1.33$, 2.33, 3.33 and 5.33, in the pump one sees a uniform flow state. The inlet and the outlet of the pump and the water in the screw part are free from backflow and bias flow, and no obvious vortex band is observed. Under the head condition of $H_0 = 4.33$, the streamlines become disordered at the inlet at 90° of the pump (Fig. 18(b)). The distribution of the streamlines in other areas of the pump is similar to that at other heads, and the streamlines in the screw section are similar. There is no abnormal streamlines in the screw part.

3.2 *Hydraulic characteristics of pump at different rotating speeds*

The rotating speed at the design head has a great influence on the hydraulic performance of the screw pump. Figure 19 shows the screw pressure distribution at different speeds (900 rpm, 1 300 rpm, 1 600 rpm, 1 900 rpm and 2 200 rpm). It can be seen from the figure that at the design rotating speed ($n = 1\,450$ rpm), the pressure of the screw gradually increases from the screw inlet in the axial direction to reach the maximum at the screw outlet surface. Under the same head condition, the screw pressure distribu-

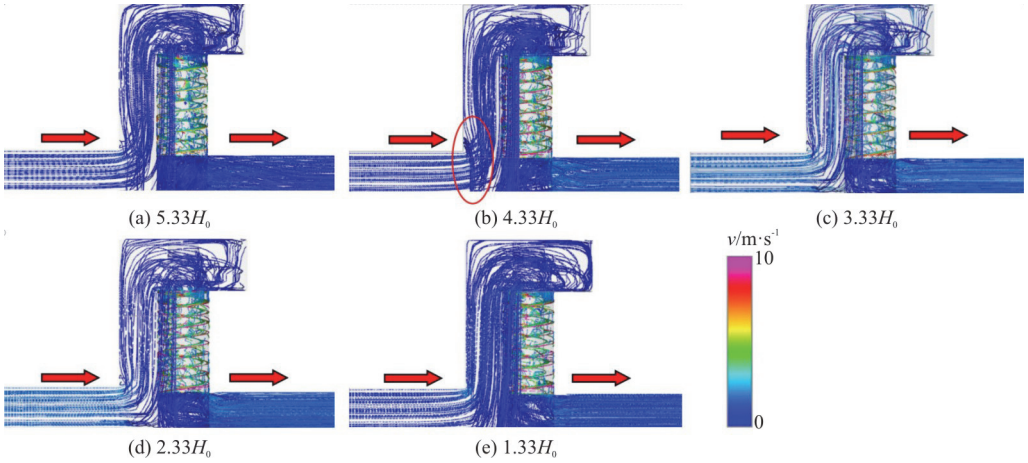

Fig. 18 (Color online) Streamlines for different heads

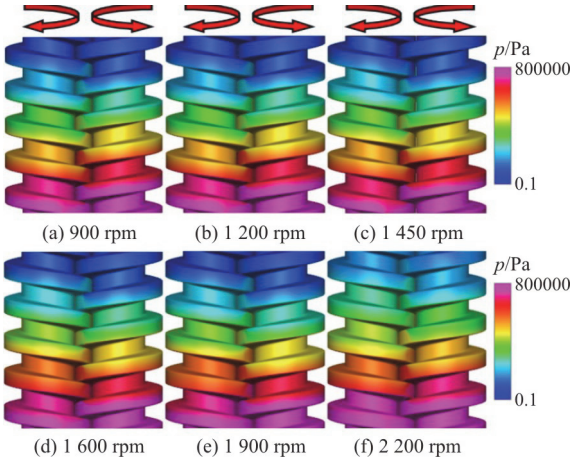

Fig. 19 (Color online) Pressure distribution of screw at different rotating speeds

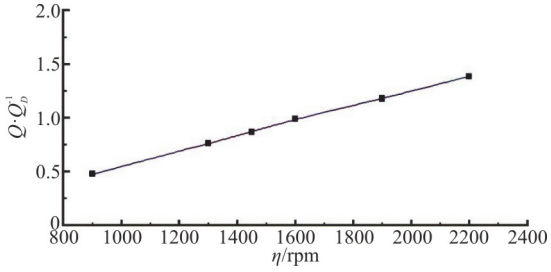

Fig. 20 Relation between rotating speeds and flow rate

tions below and above the design speed are the same as that at the design speed, with the pressure relatively close.

Figure 20 shows the corresponding relationship between the flow rate and the rotating speed of the pump. As can be seen from the figure, when the rotating speed increases, the flow rate of the pump

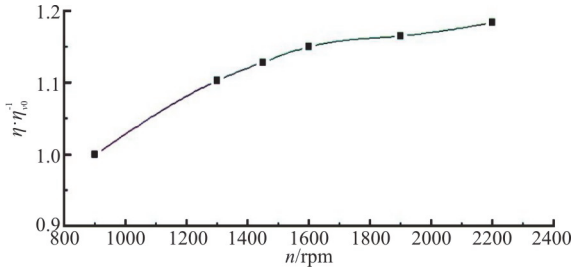

Fig. 21 Relation between rotating speed and volumetric efficiency

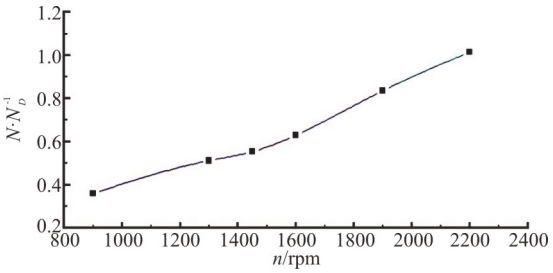

Fig. 22 Relation between rotating speeds and shaft power

rises linearly. Figure 21 shows the corresponding relationship between the volumetric efficiency and the speed of the pump. It can be seen from the figure that below the design speed, the volumetric efficiency of the pump increases with the increase of the speed. When the rotating speed is higher than the design speed, the volumetric efficiency of the pump increases with the increase of the rotating speed. Figure 22 shows the corresponding relationship between the shaft power and the rotating speed. It can be seen from the figure that when the rotating speed is lower than the design speed, the shaft power increases slowly with the increase of the speed, when the speed is higher than the design speed, the pump's shaft power

rises fast with the increase of the speed.

Figure 23 shows the flow velocity distribution in the working length of the screw at different speeds. It can be seen from the figure that as the speed increases, the flow velocity in the working length of the screw also increases. At different speeds, the flow rate distribution is the same. The flow rate is mainly uniform along the axial direction of the screw. The flow rates in the active screw and the driven screw are the same.

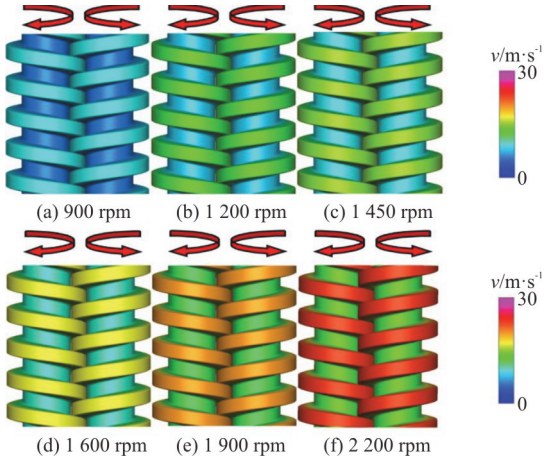

Fig. 23 (Color online) Screw flow velocity distribution at different speeds

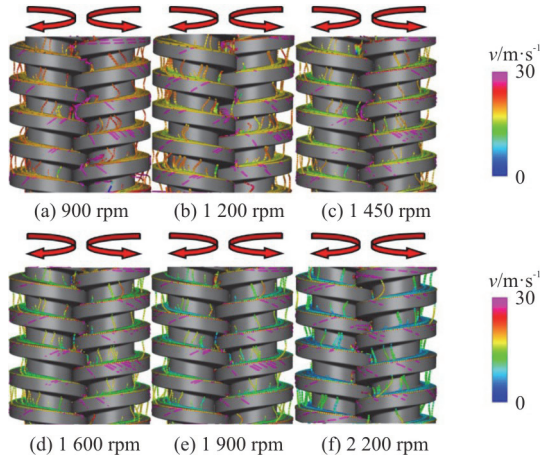

Fig. 24 (Color online) Screw streamlines at different speeds

Figure 24 shows the streamlines in the screw part at different speeds. As shown in the figure, at the design speed of 1 450 rpm, from the streamlines in the figure, one sees a velocity along the positive direction of the Z axis, indicating that the water body is recirculated, and the water body flows back from the high pressure end to the low pressure end, with a leak that can result in a loss of the pump volume. As can be seen from the figure, the leakage area is mainly concentrated in three places: the clearance between the spiral surface of the driving screw and the driven screw during the meshing process, the clearance between the screw (the rotor) and the screw bushing (the bush), the clearance between the screw addendum circle and the screw root circle. Below the design speed, the things are the same as above the design speed, the area where the leakage occurs is also concentrated in the above three clearances. With the increase of the speed, the leakage area has a diminishing trend.

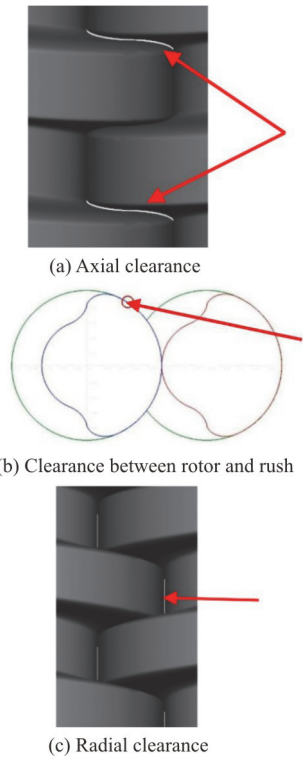

Fig. 25 (Color online) Clearances of twin-screw pump

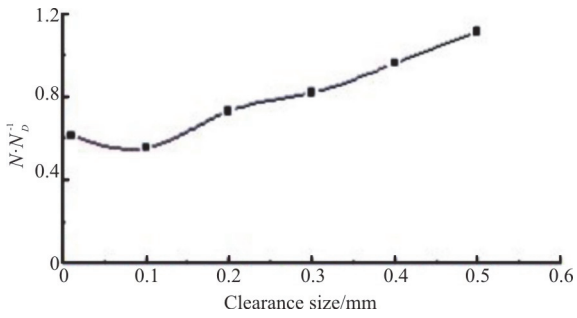

Fig. 26 Relation between axial clearance size and shaft power

4. Effect of screw clearance on hydraulic performance

There are mainly three types of clearances in the working length of the Ω-type twin-screw pump, As shown in Fig. 25: the axial clearance between the spiral surfaces of the male and female rotors during

the meshing process, the clearance between the tooth tip of the screw rotor and the screw bushing and the radial clearance between the tooth tip and the tooth root. For the above three kinds of clearances, the unreasonable design of the clearance size will affect the normal operation of the screw pump. According to previous studies, the clearance of the screw surface has the greatest influence on the performance of the pump, and the other clearances have less influence. Therefore, the effect of the axial clearance size on the hydraulic performance of the pump should be studied.

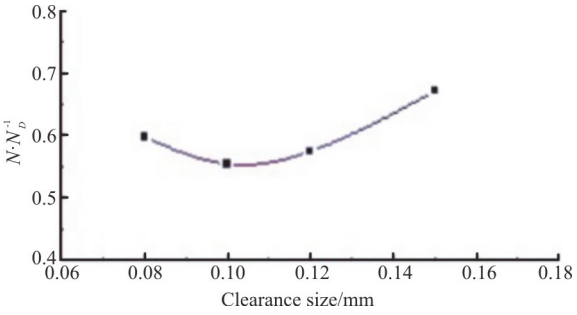

Fig. 27 Relation between axial clearance size and shaft power

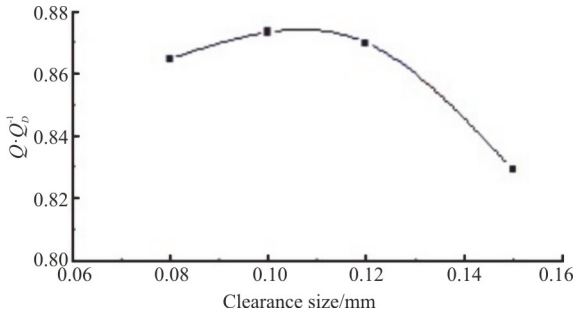

Fig. 28 Relation between axial clearance size and flow rate

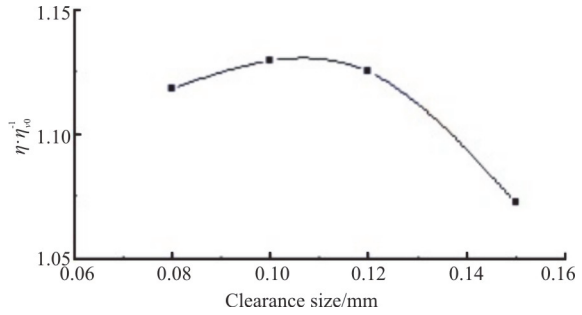

Fig. 29 Relation between axial clearance size and volumetric efficiency

4.1 *Selection of axial clearance size*

As the axial clearance of the screw has a great influence on the performance of the pump, the hydraulic performance of the pump under different axial clearances is simulated by the CFD and the twin-screw clearance is optimized. First, the axial clearance values are selected in a relatively wide range, which are 0.01 mm, 0.10 mm, 0.20 mm, 0.30 mm, 0.40 mm and 0.50 mm. Figure 26 shows the variation of the shaft power for different clearances. As can be seen from the figure, the shaft power is minimal when the axial clearance size is 0.10 mm. When the clearance size is greater than 0.20 mm, the shaft power increases more quickly.

According to the calculation results of the above scheme, the shaft powers for the four axial clearances (0.08 mm, 0.10 mm, 0.12 mm, and 0.15 mm) are shown in Fig. 27. When the clearance is 0.08 mm, 0.10 mm and 0.12 mm, the shaft power takes relatively close values and lower than the shaft power under the clearance of 0.15 mm. Figure 28 shows the relationship between the clearance and the flow rate, and Fig. 29 shows the relationship between the clearance and the volumetric efficiency. It can be seen from the figure that when the axial clearance is 0.10 mm, the flow rate takes the maximum value and the volumetric efficiency is the highest. When the axial clearance is 0.15 mm, the flow rate is the smallest and the volumetric efficiency is the lowest.

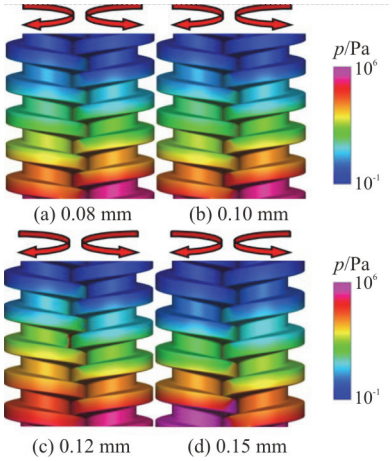

Fig. 30 (Color online) Screw pressure distribution for different axial clearance sizes

Figure 30 shows the screw pressure diagram at axial clearances of 0.08 mm, 0.10 mm, 0.12 mm and 0.15 mm. As can be seen from the figure, with different axial clearance sizes, the screw pressure distributions are roughly the same, increasing gradually from the inlet surface of the screw in the axial direction, with the smallest at the inlet surface of the screw, and the largest at the outlet surface. When the axial clearance is 0.08 mm, 0.10 mm, the screw pressure in the same area is relatively close. With the clearance sizes of 0.08 mm, 0.10 mm, and 0.12 mm, the maximum pressure of the male rotor is lower than that of the female rotor, and when the axial clearance

size is 0.15 mm, the maximum pressure of the male rotor is higher than that of the female rotor.

Figure 31 shows the screw streamlines for different axial clearance sizes. It can be seen from the figure that there are streamlines from the high pressure side to the low pressure side near the meshing area between the male rotor and the female rotor, which means that a leak has occurred.

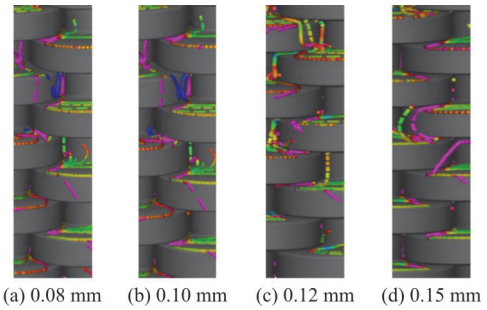

Fig. 31 (Color online) Streamlines for different axial clearance sizes

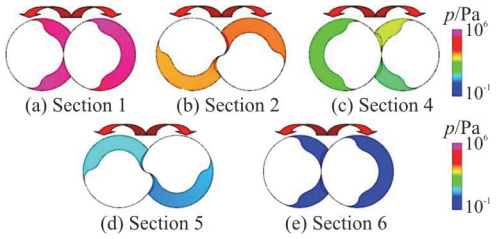

Fig. 32 (Color online) Screw pressure distribution in different sections

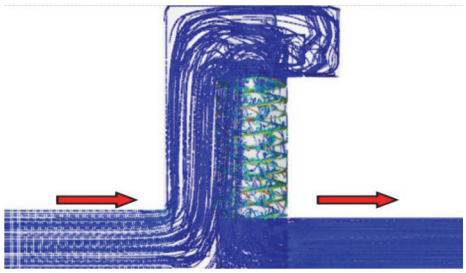

Fig. 33 (Color online) Streamlines for axial clearance of 0.10 mm

In summary, we have considered the hydraulic performance, the manufacturing process and other factors, for the axial clearance size of 0.10 mm. The pressure of the screw end faces in different sections under this clearance size is shown in Fig. 32. From the figure, we can see that, in addition to the Section 4 ($Z = 0.20$), the female rotor pressure is slightly higher than that of the male rotor, In the other Sections, the pressure distributions of the male rotor and the female rotor are basically the same, and the pressure value is close. Section 6 is the inlet surface of the screw. The section pressure is negative, and the remaining section pressure is positive. Figure 33 shows the streamlines in the pump with the clearance of 0.10 mm. It can be seen from the figure that the flows in the pump inlet and outlet are smooth, with no vortex and bias flow. The flow of the water in the screw part is complicated, but no bad flow pattern occurs.

4.2 *Selection of clearance size between rotor and bush*

For the clearance between the screw rotor and the bush, that is, the clearance between the screw and the bushing, its size is selected according to the empirical formula: $0.015\sqrt{R_1}$.

4.3 *Selection of clearance size between addendum circle and dedendum circle*

The clearance size between the addendum circle and the dedendum circle can be selected from 0.08mm to 0.15mm based on experience. The best axial clearance of 0.10 mm is suggested.

5. Conclusions

(1) Under different head conditions, the flow rate of the twin-screw pump decreases with the increase of the head. The screw pressure gradually increases from the inlet end face along the axial direction of the screw to the outlet end face, and the pressure near the screw inlet end face is negative. The pressure distribution in the screw groove is relatively uniform, but the pressure distributions in the screw clearance and the meshing area are different from that in the screw groove.

(2) As the speed increases, the pump flow rate increases in a straight line. Below the design speed, the volumetric efficiency of the pump increases significantly with the increase of the rotating speed, while the shaft power increases slowly. When the rotating speed is higher than the design speed, the volumetric efficiency of the pump increases slowly with the increase of the speed, while the shaft power increases rapidly.

(3) It is shown that the designed screw pump enjoys higher efficiency and lower shaft power when the axial clearance is 0.08 mm-0.12 mm. The actual flow rate is divided by the theoretical flow rate to obtain the volumetric efficiency. When the clearance is around 0.1 mm, the volumetric efficiency is the highest.

(4) Tests show that the head of the twin-screw pump tends to decrease with the increase of the flow rate at different speeds. Under the same head condition, the pump flow rate increases with the increase of the rotating speed. The efficiency of the screw pump increases significantly with a decrease of the flow rate within a certain range. When running

near the high efficiency area of the pump, the efficiency of the pump increases slowly as the flow rate decreases. Numerical simulations and experimental results are basically consistent.

Acknowledgments

This work was supported by the Innovation Capability Planning Project-Colleges and Universities Cooperation Project (Grant No. YZ2017289), the Postgraduate Research and Practice Innovation Program of Jiangsu Province (Grant No. XKYCX19_089), the Six talent peaks project in Jiangsu Province (Grant No. 2015-JXQC-007), the Water conservancy science and technology project of Jiangsu Province (Grant No. 2019014), the Priority Academic Program Development of Jiangsu Higher Education Institutions (PAPD) and the Jiangsu Province 333 high level talents training project and Jiangsu Planned Projects for Postdoctoral Research Funds (Grant No. 1701189B).

References

[1] Li F. Screw pump [M]. Beijing, China: Machine Press, 2010(in Chinese).

[2] Yan D., Tang Q., Kovacevic A. et al. Rotor profile design and numerical analysis of 2-3 type multiphase twin-screw pumps [J]. *Proceedings of the Institution of Mechanical Engineers, Part E: Journal of Process Mechanical Engineering*, 2018, 232(2): 186-202.

[3] Liu P., Morrison G., Patil A. Experimental and analytical investigation of a novel multistage twin-screw pump [J]. *Journal of Energy Resources Technology*, 2019, 141(12): 122101.

[4] An Y., Song Y., Zhang D. et al. Three dimensional motion simulation and locus optimization design of progressive cavity pump rotor [J]. *Journal of China University of Petroleum (Edition of Natural Science)*, 2012, 36(3): 155-158, 164(in Chinese).

[5] Wang J., Wei S., Sha R. et al. Design methodology of a new smooth rotor profile of the screw vacuum pump [J]. *Vacuum*, 2019, 159: 456-463.

[6] Li Z., Zhang R., Gao Y. et al. Profile analysis and simulation of twin-screw pump [J]. *China Petroleum Machinery*, 2008, 36(3): 41-44(in Chinese).

[7] Chen J., Wang L., Chen D. Revise of double-screw pump profile [J]. *Fluid Machinery*, 2006, 34(6): 41-43.

[8] Tang Q., Zhang Y. Screw optimization for performance enhancement of a twin-screw pump [J]. *Proceedings of the Institution of Mechanical Engineers*, 2014, 228(1): 73-84.

[9] Yan D., Kovacevic A., Tang Q. Numerical modelling of twin-screw pumps based on computational fluid dynamics [J]. *Proceedings of the Institution of Mechanical Engineers*, 2017, 231(24): 4617-4634.

[10] Ohbayashi T., Sawada T., Hamaguchi M. Study on the performance prediction of screw vacuum pump [J]. *Applied Surface Science*, 2001, 169: 768-771.

[11] Zhang H. Y., Zhang W. Y., Zhu D. P. Study on design of twin- screw pump with high pressure water [J]. *Ship Engineering*, 2015, S1: 117-118(in Chinese).

[12] Hu B., Cao F., Yang X. Theoretical and experimental study on conveying behavior of a twin-screw multiphase pump [J]. *Proceedings of the Institution of Mechanical Engineers*, 2016, 230(4): 304-315.

[13] Liu P., Patil A., Morrison G. Multiphase flow performance prediction model for twin-screw pump [J]. *Journal of Fluids Engineering*, 2018, 140(3): 031103.

[14] Zhang Y., Tang Q., Li Z. et al. Leakage mechanism of screw pump based on leakage model in fluid mechanics [J]. *Transactions of the Chinese Society for Agricultural Machinery*, 2014, 45(10): 326-332, 339(in Chinese).

[15] Zhang Y. Investigation on the design and manufacuture processing technology of sealed twin-screw rotor [D]. Master Thesis, Chongqing, China: Chongqing University, 2010(in Chinese).

[16] Zhang Y. Characteristic analysis of volumetric efficiency and precision forming research of rotors for screw pump [D]. Doctoral Thesis, Chongqing, China: Chongqing University, 2014(in Chinese).

[17] Patil A. Performance evaluation and CFD simulation of multiphase twin-screw pumps [D]. Doctoral Thesis, College Station, TX, USA: Texas A&M University, 2013.

[18] Yin X., Cao F., Pan S. Numerical investigation on screw rotor deformation and influence on volumetric efficiency of the twin-screw multiphase pump [J]. *Applied Thermal Engineering*, 2017, 111(25): 1111-1118.

[19] Wang X. Design theory and simulation study of water hydraulic twin-screw pump with medium and high pressure [D]. Master Thesis, Chongqing, China: Chongqing University, 2014(in Chinese).

[20] Chu T., Wang C., Wang X. et al. Numerical simulation study of screw pump internal flow field [J]. *Fluid Machinery*, 2014, 42(5): 21-24.

[21] Wang C., Chen X., Qiu N. et al. Numerical and experimental study on the pressure fluctuation, vibration, and noise of multistage pump with radial diffuser [J]. *Journal of the Brazilian Society of Mechanical Sciences and Engineering*, 2018, 40(10): 481.

[22] Wang C., Shi W., Wang X. et al. Optimal design of multistage centrifugal pump based on the combined energy loss model and computational fluid dynamics [J]. *Applied Energy*, 2017, 187: 10-26.